Enhanced reforming of mixed biomass tar model compounds using a hybrid gliding arc plasma catalytic process

Danhua Mei [1,2], Shiyun Liu [1,2], Yaoling Wang[1], Haiping Yang[3], Zheng Bo[4], Xin Tu [1,*]

[1] *Department of Electrical Engineering and Electronics, University of Liverpool, Liverpool L69 3GJ, UK*

[2] *College of Electrical Engineering and Control Science, Nanjing Tech University, Nanjing 211816, Jiangsu, China*

[3] *State Key Laboratory of Coal Combustion, School of Energy and Power Engineering, Huazhong University of Science and Technology, Wuhan 430074, China*

[4] *State Key Laboratory of Clean Energy Utilization, Institute for Thermal Power Engineering, College of Energy Engineering, Zhejiang University, Hangzhou 310027, China*

*** Corresponding Author**

Dr. Xin Tu

Department of Electrical Engineering and Electronics,

University of Liverpool,

Liverpool, L69 3GJ,

UK

Tel: +44-1517944513

E-mail: xin.tu@liv.ac.uk

Abstract

Plasma-catalytic steam reforming of mixed tar model compounds (toluene and naphthalene) from biomass gasification has been carried out in a gliding arc discharge (GAD) plasma reactor. The influence of three catalysts (15Ni, 7.5Ni7.5Co and 15Co) on the performance of the plasma reforming of toluene and naphthalene has been evaluated including the conversion, the energy efficiency, the yield/selectivity of gaseous products and the formation of by-products. A plasma-catalysis synergy was generated when introducing the catalysts to the plasma tar reforming process. The highest toluene conversion of 95.7% and naphthalene conversion of 83.4% were achieved when the 7.5Ni7.5Co catalyst was integrated with the GAD plasma at a total tar concentration of 16.0 g/Nm^3 and a discharge power of 75 W. The corresponding energy efficiency for the conversion of toluene and naphthalene was 38.0 g/kWh and 2.3 g/kWh, respectively, giving the highest total tar conversion of 95.1% and overall energy efficiency of 40.3 g/kWh. The coupling of GAD with the 7.5Ni7.5Co catalyst also showed the highest yield of H_2 (42.3%) and CO (37.3%) and the highest CO selectivity of 40.1%. In addition, the combination of the GAD plasma with 7.5Ni7.5Co reduced the carbon deposition on the catalyst surfaces and the formation of by-products in the plasma-catalytic tar reforming process. The enhanced reducibility and NiCo alloy formation of the 7.5Ni7.5Co catalyst contribute to the enhanced conversion of mixed tar compounds and the formation of the plasma-catalysis synergy in the hybrid plasma-catalytic tar reforming process.

Keywords: Non-thermal plasmas; Gliding arc; Biomass gasification tar; Plasma-catalysis; Synergistic effect

1. Introduction

Biomass conversion and utilization has been regarded as one of the most promising solutions to deal with the increasing energy demand from the growing population and the climate change caused by the rapid consumption of fossil fuels [1]. Thermochemical conversion of biomass via gasification is an attractive process to produce syngas (a mixture of hydrogen and carbon monoxide), which is a key chemical feedstock for the production of liquid hydrocarbons and oxygenates [2, 3]. However, the formation of problematic tars in biomass gasification remains a significant barrier to limit the further development and commercialization of biomass gasification technology. Tar consists of mixed condensable aromatic hydrocarbons such as single-to-polycyclic aromatic hydrocarbons (PAHs). Some of the tar compounds are harmful to human beings due to their carcinogenicity [4]. The formed tars in biomass gasification can condense in fuel lines, filters and engine channels when cooled in the downstream of the gasification system, which leads to contamination, clogging and corrosion in processing units, resulted in the increased maintenance costs and decreased energy efficiency[5]. Therefore, tar removal is essential and crucial for the effective utilization of the fuel gas derived from biomass gasification.

A variety of approaches have been investigated to eliminate tars from gasification, including physical processes (e.g., mechanical separation [6, 7]), thermal cracking [8] and catalytic reforming [9-12]. Physical processes for tar removal usually lead to the waste of carbon energy resources, the secondary pollution and the additional cost for disposing of the collected tars. Thermal cracking is an energy-intensive process as high temperatures (>1000 ^{o}C) are required to achieve reasonable tar conversion. Catalytic reforming is an attractive process to convert tars into syngas at relatively low temperatures (750-900 ^{o}C). Different catalysts have been tested in the catalytic reforming of tars, such as supported transition metal (e.g., Ni, Co and Fe) and noble metal (e.g. Rh, Ru and Pt) catalysts, metal oxides (e.g. ferrous metal oxides and

activated alumina) and natural mineral catalysts (e.g. olivine, dolomite and ceramic-based catalysts). [13, 14]. Among these catalysts, supported transition metal catalysts, especially Ni-based catalysts have been extensively used in the catalytic reforming of tars due to their high activity, availability and low cost [12]. However, catalyst deactivation due to catalyst sintering and carbon fouling remains a major challenge in the catalytic reforming of tars. Adding cobalt to Ni catalysts has great potential to suppresses carbon deposition due to possible synergistic interactions between Ni and Co species, compared to monometallic Co and Ni catalysts. This effect has been demonstrated in catalytic CO_2 reforming of CH_4 [15].

Non-thermal plasma (NTP) technology provides an unconventional but promising solution for the effective removal of biomass gasification tars at low temperatures [16-19]. Different non-thermal plasmas have been developed for the conversion of tars, including corona discharge [20, 21], dielectric barrier discharge (DBD) [22, 23], gliding arc discharge (GAD) [24-26] and microwave discharge [27, 28]. However, the yield and selectivity of the target products need to be further improved to enhance the overall energy efficiency of the plasma processes [16]. In addition, a trade-off between the conversion of tar and energy efficiency remains a major challenge to achieve high conversion and energy efficiency simultaneously in plasma-based chemical processes.

The coupling of NTP with heterogeneous catalysis, known as plasma-catalysis has great potential to overcome the trade-off between the conversion and energy efficiency of plasma chemical processes. Catalyst can be placed either in the plasma zone to form in-plasma catalysis (IPC) or in the downstream the plasma region to form a post-plasma catalysis (PPC) configuration [29-32]. Integrating catalysts into a plasma induces mutual interactions between the plasma and the catalyst, upon which a synergistic effect could be generated with high potential, leading to the enhanced the conversion of reactants, the yield and selectivity of the specific products and the energy efficiency of the process [33]. Numerous studies have

demonstrated the effectiveness of using a hybrid plasma-catalytic process for the removal of gas pollutants [19, 34], the synthesis of fuels and chemicals [16, 35, 36], and the treatment of catalysts [37]. In our previous work, we investigated plasma-catalytic steam reforming of toluene as a tar surrogate using a DBD reactor. The results showed that placing a Ni/Al_2O_3 catalyst in the DBD reactor significantly enhanced the conversion of toluene, the yield of H_2 and the overall energy efficiency of the plasma tar reforming process. In addition, the Ni/Al_2O_3 catalyst with a higher Ni loading showed higher reaction performance [16]. Liu et al. found that packing a Ni/Al_2O_3 catalyst into a DBD reactor promoted the plasma reforming of toluene at a constant heating temperature of 300 ^oC with the highest toluene conversion of 96% and the energy efficiency of 20 g/kWh [22]. Xu et al. investigated the plasma-catalytic reforming of toluene in a temperature-controlled DBD reactor. The highest energy efficiency for toluene conversion was achieved with a high toluene conversion when a $Ni/\gamma\text{-}Al_2O_3$ catalyst was placed in the plasma reaction at an optimal heating temperature of 400 ^oC [23]. DBD plasma reactors have been commonly used for plasma-catalytic processes due to its flexibility of combining DBD with solid catalysts in different ways. Although a range of catalysts has been tested in plasma-catalytic oxidation of volatile organic compounds (VOCs) and greenhouse gas conversion, far less has been done for the reforming of tar surrogates. Additionally, the treatment capability (e.g., the concentration of tars) and energy efficiency in the DBD-based plasma-catalytic process were much lower compared with those using gliding arc plasmas even without a catalyst [33]. Previous works have shown that GAD plasma is very effective for the conversion of a range of carbon sources including biomass tars for the synthesis of fuels and chemicals compared to DBD systems [16, 38, 39]. Integrating suitable catalysts into a GAD reactor has great potential to further enhance the performance of plasma chemical reactions [33]. However, limited works have focused on the combination of GAD with catalysts for chemical reactions [33, 40], especially biomass tar reforming. Understanding the influence of

catalysts on the reforming of tars in a GAD reactor is indispensable and the key to further enhance the performance of GAD plasma-catalytic reforming process.

In this work, a GAD-based hybrid plasma-catalytic process has been developed for steam reforming of mixed toluene and naphthalene, typical light monoaromatic and polycyclic aromatic tar compounds with high thermal stability from the biomass gasification. The effect of different catalysts (15Ni, 15Co and 7.5Ni7.5Co) supported on γ-Al_2O_3 was evaluated to understand their effects on the conversion of tar compounds, the energy efficiency of the hybrid process and the yield and selectivity of gas products. Moreover, the plausible reaction mechanism involved in the plasma-catalytic process was elucidated based on a comprehensive analysis of the gaseous and liquid products coupled with the characterization of the catalysts before and after the reaction.

2. Experimental

2.1 Catalysts preparation and characterization

The x wt.%Ni- y wt.%Co/γ-Al_2O_3 (x = 0, 7.5 and 15; x + y = 15) catalysts were prepared by the wetness impregnation method (co-impregnation for bimetallic catalyst) using nitrates ($Ni(NO_3)_2 \cdot 6H_2O$ and $Co(NO_3)_2 \cdot 6H_2O$, Alfa Aesar) as metal precursor. The appropriate weight of γ-Al_2O_3 powder was added to the solution of the metal precursor and impregnated for 4 hours. The obtained samples were dried at 110 ^oC for 12 h, and then calcined at 500 ^oC for 5 h. Prior to the plasma reforming reaction, the calcined catalysts were thermally reduced in 25 vol. %H_2/Ar at 600 ^oC for 2 h. The obtained catalyst samples were denoted as 15Ni, 7.5Ni7.5Co and 15Co.

The X-ray powder diffraction (XRD) patterns of the calcined and reduced catalyst samples were recorded using an Empyrean X-ray diffractometer equipped with Mo and Ag sources (60 kV tube voltage and 40 mA tube current) in the scanning range 2θ between 5^o and 80^o with a scanning rate of 4 ^{o}/min. The N_2 physisorption was carried out at 77 K on a Quantasorb surface area analyzer (Micromeritics, ASAP2000, USA). The surface area of the catalysts was

estimated using the Brunauer-Emmett-Teller (BET) method, while the total pore volume and average pore diameter of the catalysts were determined by the Barrett-Joyner- Halenda (BJH) method. Hydrogen temperature-programmed reduction (H_2-TPR) was carried out in 10 vol. % H_2/Ar in the temperature range of 20-800 ^oC with a heating rate of 5 ^oC/min using a Micromeritics Autochem 2920 instrument. The carbon deposition on the spent catalysts was determined via thermal gravimetric analysis (TGA) in the air using a TA Instruments SDT-Q600.

2.2 Experimental setup

Plasma reforming of tar model compounds was carried out in a GAD reactor with two knife-shaped stainless-steel electrodes, as shown in Fig. 1. More details of the reactor configuration can be found in our previous work [17]. Nitrogen was used as carrier gas (BOC, 99.999% purity). A mixed stream of naphthalene (purity >= 99%, Aldrich), toluene (purity >= 99%, Aldrich), deionized water and carrier gas was preheated to 300 ^oC in a tube furnace before injecting to the GAD reactor. In this work, the concentration of toluene and naphthalene was fixed at 15.0 and 1.0 g /Nm^3, respectively, while the total flow rate of the feed mixture was kept constant at 3.5 L/min with a steam/carbon (S/C) ratio of 1.5. The GAD reactor was connected to a high voltage neon transformer with a constant frequency of 50 Hz. The discharge power can be controlled by changing the applied voltage from 0 to 10 kV. The arc voltage and arc current were measured by a high voltage probe (Testec, TT-HVP 15 HF) and a current monitor (Magnelab, CT-E 0.5-BNC), respectively. A four-channel digital oscilloscope (Tektronix, MDO 3024) was used to monitor and record the voltage and current signals. A catalyst bed (1 g catalyst) was placed in the downstream of the electrode end and contacted with the gliding arc. The temperature of the catalyst bed in the plasma reforming of tars was measured using a thermocouple (Fig. 1). Fig. 2 shows the temperature of the catalyst bed was almost constant (~360 ^oC) after running the experiment for around 12 mins at a discharge power of 75 W when using the 7.5Ni7.5Co catalyst. Using different catalysts did not change the temperature of the catalyst bed (~360 ^oC) in this experiment. In the absence of the catalyst bed,

the temperature of the gliding arc in the same position was slightly lower (~352 ^{o}C) due to the inelastic electron-molecule collisions in the plasma-catalytic reaction [36, 41].

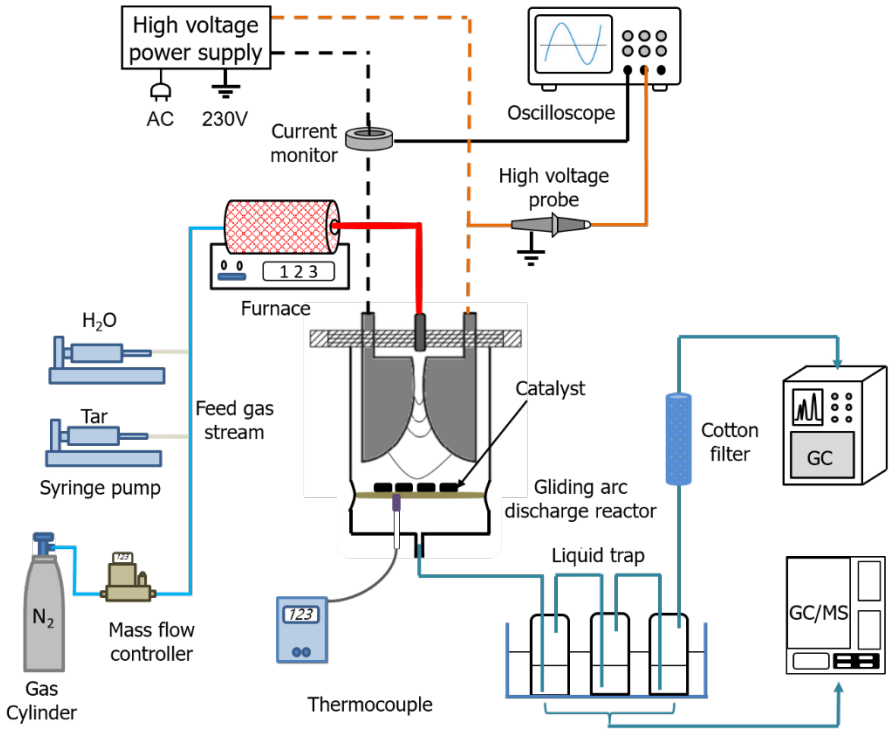

Fig.1 Schematic diagram of the experimental setup

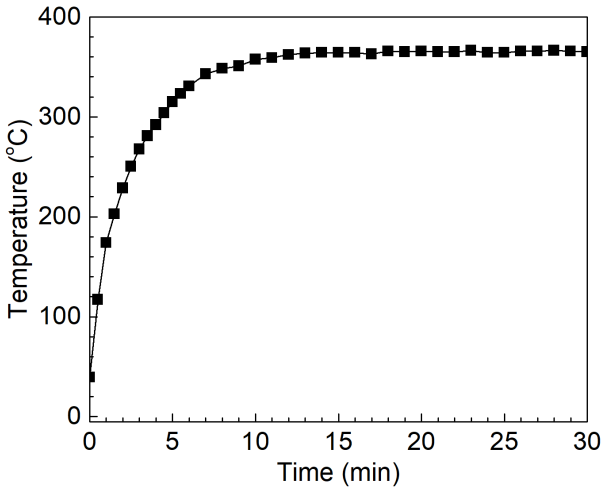

Fig. 2. Temperature of the catalyst bed as a function of time (C_7H_8 content: 15.0 g/Nm^3; $C_{10}H_8$ content: 1.0 g/Nm^3; Discharge power: 75 W; Q: 3.5 L/min; S/C molar ratio: 1.5; Catalyst: 7.5Ni7.5Co)

To understand the synergistic effect of the plasma-catalyst coupling in the reforming of tar model compounds, catalytic reforming of toluene and naphthalene over 10Ni, 7.5Ni7.5Co and 10Co was also carried out at 360 ^{o}C with all the other conditions kept the same for the plasma reaction.

2.3 Method of analysis and the definition of parameters

The gas products were analyzed by using two-channel gas chromatography (Shimadzu, GC-2014). An ice-cold trap including three successive absorption bottles was used for collecting unconverted tars and condensable products. The first two bottles contain dichloromethane (DCM) to absorb condensable products, and the last bottle was kept empty to collect remaining entrained droplets. The condensed liquid products were detected by an Agilent GC - mass spectrometry (GC/MS, Agilent GC 7820A-5975C) and analyzed using the standard library of the NIST (National Institute of Standards and Technology).

In the plasma tar reforming reaction, the conversion of tar X_{tar} can be calculated by Eq. (1):

$$X_{\text{tar}}(\%) = \frac{C_o - C_i}{\mathrm{C_i}} \times 100 \tag{1}$$

where C_i and C_o are the concentration of tar (toluene or naphthalene) before and after the reaction, respectively.

The yield and selectivity of the gas products are defined by Eq. (2) - (6). As we cannot measure the conversion of H_2O in this study, the selectivity of H_2 cannot be determined.

$$Y_{\mathrm{H_2}}(\%) = \frac{(\mathrm{H_2})_{\text{produced}}(\mathrm{mol/s})}{4\times(\mathrm{C_7H_8}+\mathrm{C_{10}H_8})_{\text{input}}(\mathrm{mol/s})+\mathrm{H_2O}_{\text{input}}(\mathrm{mol/s})} \times 100 \tag{2}$$

$$Y_{\mathrm{CO_x}}(\%) = \frac{(\mathrm{CO_x})_{\text{produced}}(\mathrm{mol/s})}{(7\times\mathrm{C_7H_8}+10\times\mathrm{C_{10}H_8})_{\text{input}}(\mathrm{mol/s})} \times 100 \tag{3}$$

$$S_{CO_x}(\%) = \frac{(CO_x)_{produced}(mol/s)}{(7\times C_7H_8 + 10\times C_{10}H_8)_{converted}(mol/s)} \times 100 \quad (4)$$

$$Y_{C_xH_y}(\%) = \frac{(x\times C_xH_y)_{produced}(mol/s)}{(7\times C_7H_8 + 10\times C_{10}H_8)_{input}(mol/s)} \times 100 \quad (5)$$

$$S_{C_xH_y}(\%) = \frac{(x\times C_xH_y)_{produced}(mol/s)}{(7\times C_7H_8 + 10\times C_{10}H_8)_{converted}(mol/s)} \times 100 \quad (6)$$

The energy efficiency *E* of the plasma reforming process is defined as the mass of converted tar per unit of discharge power, shown in Eq. (7).

$$E(g/kWh) = \frac{\text{mass of converted tar (g/h)}}{\text{Discharg power (kW)}} \quad (7)$$

A synergistic capacity (SC) of the plasma-catalytic process is introduced to evaluate the effect of the catalysts on the plasma reforming of tars [42]:

$$SC_{\xi}(\%) = \frac{\xi_{p+c} - \xi_p - \xi_c}{\xi_p + \xi_c} \times 100 \quad (8)$$

where ζ can be the conversion of tar, the yield and selectivity of gas products and the energy efficiency. The subscripts p+c, p and c, represent the results from plasma-catalysis, plasma-only and catalyst-only, respectively.

3. Results and discussion

3.1 Catalyst characterization

The BET specific surface area of γ-Al_2O_3 and the reduced catalysts are summarized in Table 1. Compared to the BET specific surface area of 15Ni (201.4 m^2/g) and 15Co (172.8 m^2/g), a larger specific surface area of 224.9 m^2/g was obtained for 7.5Ni7.5, which is beneficial to the tar reforming as larger surface area could provide more active sites on the catalyst surface. The pore volume of the catalysts (0.37 – 0.45 cm^3/g) was smaller than that of γ-Al_2O_3 (0.54 cm^3/g),

which could be attributed to the partial coverage of γ-Al_2O_3 pores by deposited metals [43, 44]. Loading active metals on catalyst support would result in the clogging of micropores of the support while leaving meso- and macro-pores unaffected [44], which leads to the higher average pore diameter of the reduced catalysts compared to that of γ-Al_2O_3, as shown in Table 1.

Table 1. Physicochemical properties of γ-Al_2O_3 and reduced catalysts.

Sample	Specific surface area (m^2/g)	Pore volume (cm^3/g)	Average pore diameter (nm)
γ-Al_2O_3	368.0	0.54	5.45
15Ni	201.4	0.41	6.53
7.5Ni7.5Co	224.9	0.45	6.38
15Co	172.8	0.37	6.74

Fig. 3 shows the XRD patterns of the catalyst support, calcined and reduced catalysts. For γ-Al_2O_3, typical diffraction peaks can be clearly observed at 2θ = 14.5°, 28.3°, 38.5°, 45.8°, 49.7° and 67.1°. These peaks can also be identified in the XRD patterns of the reduced catalysts. However, the intensities of γ-Al_2O_3 peaks in the XRD of the reduced catalysts were much lower than that of the support. The diffraction peaks of Co_3O_4 and NiO were shown in the calcined 15Co and 15Ni catalysts (see Fig. 3 (a)), respectively, which indicates the formation of metal oxide crystallites. No characteristic peaks of $NiAl_2O_4$ and $CoAl_2O_4$ can be observed in the calcined catalysts, which might be attributed to the overlap of diffraction peaks of the cubic spinel species with that of the cubic phase NiO and the spinel phase Co_3O_4 [45, 46]. For the reduced 15Ni catalyst (see Fig.3 (b)), the diffraction peaks at 2θ = 44.6°, 51.8° and 76.5° can be assigned to the diffraction of Ni metal phase; while the diffraction peaks at 2θ = 44.2°, 51.4° and 75.7° in the XRD pattern of the 15Co catalyst indicates the existence of elemental Co [47]. The reduced 7.5Ni7.5Co catalyst displayed a similar XRD pattern as that of the 15Ni and 15Co catalysts. Fig.3(c) shows the X-ray patterns of the catalysts after reduction in a narrow range of 2θ. Clearly, the XRD pattern of the reduced 7.5Ni7.5Co catalyst exhibited only one

diffraction peak at 44.4°, suggesting the formation of Ni-Co alloy in the bimetallic 7.5Ni7.5Co catalyst after the reduction [48]. Similar results were reported in previous studies [49-51].

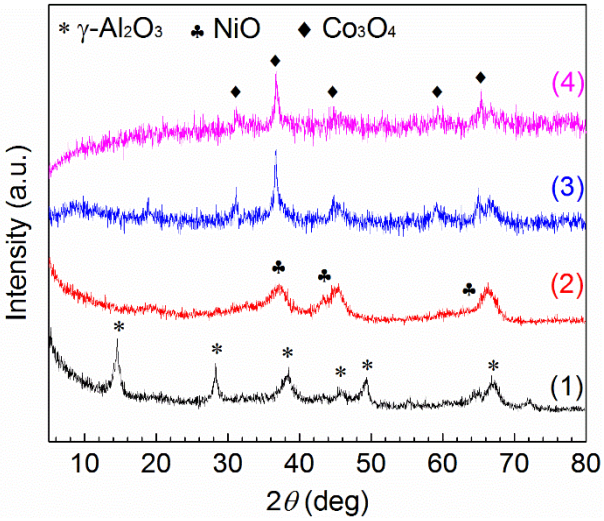

(a)

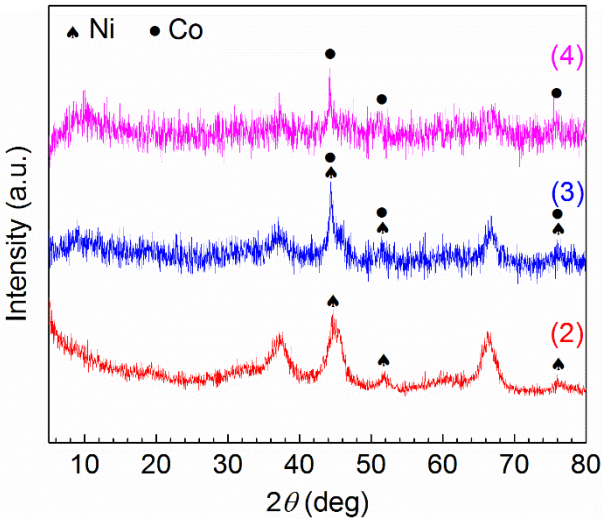

(b)

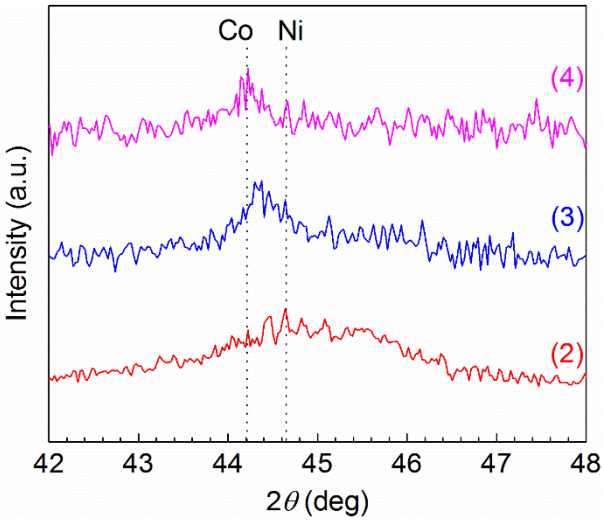

(c)

Fig. 3. XRD patterns of (a) γ-Al_2O_3 support and calcined catalysts (b) the reduced catalysts before the reaction and (c) the reduced catalysts with 2θ range of 42° – 48°: (1) γ-Al_2O_3; (2) 15Ni; (3) 7.5Ni7.5Co; (4) 15Co.

The reducibility of the catalysts was evaluated by H_2-TPR, as shown in Fig. 4. The 15Ni catalyst exhibited two major peaks centered at 413.3 ^oC and 638.5 ^oC. The first peak can be attributed to the reduction of bulk NiO, while the second one suggests the reduction of NiO which had a medium-strength interaction with γ-Al_2O_3. H_2 consumption of the 15Ni catalyst also occurred at a temperature of >700 ^oC, indicating the formation of $NiAl_2O_4$ which can only be reduced at high temperatures (>700 ^oC) [17, 44]. The H_2-TPR profile of the 15Co catalyst showed a notable peak at 311.3 ^oC and a broad peak at around 408.8 ^oC, revealing that Co oxides were reduced through two steps. The first peak is associated with the reduction of Co_3O_4 to CoO, while the second one suggests the further reduction of CoO to elemental Co [49, 52]. Compared to the 15Ni and 15Co catalysts, the reduction of the 7.5Ni7.5Co catalyst started at a lower temperature of 266.7 ^oC. Such a shift of the reduction peak to a lower temperature indicates enhanced reducibility of the 7.5Ni7.5Co catalyst, suggesting that the presence of Co decreased the reduction temperature of surface metal oxide species. A similar finding was reported in catalytic steam reforming of ethanol using similar Ni/Al_2O_3, Co/Al_2O_3 and bimetallic Ni-Co/Al_2O_3 catalysts [47]. In this study, the 7.5Ni7.5Co catalyst exhibited the strongest reducibility, followed by the 15Co and 15Ni catalyst.

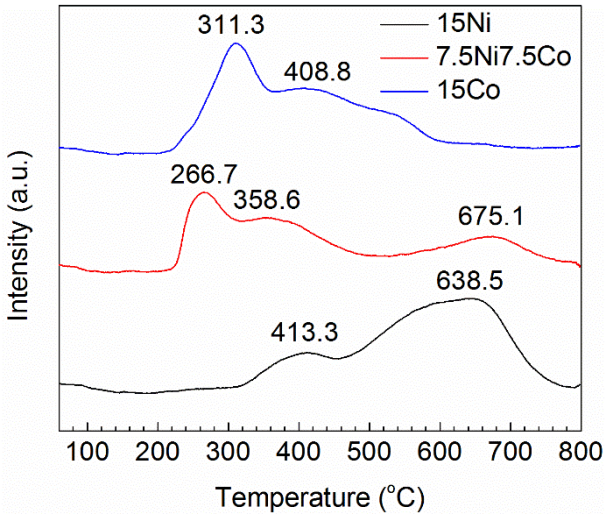

Fig. 4. H_2-TPR patterns of fresh 15Ni, 7.5Ni7.5Co and 15Co catalysts

3.2 Plasma-catalytic reforming of tars

Fig. 5 shows the effect of different catalysts on the conversion of toluene and naphthalene, as well as the energy efficiency of the plasma reforming process. The conversion of toluene was significantly higher than that of naphthalene even though the concentration of naphthalene was only 1/15 of the concentration of toluene. Compared to the dissociation of naphthalene in the GAD plasma, the initiate reaction (H-abstraction) for toluene destruction is more effective due to the presence of a methyl group in toluene. A similar finding was also reported by Nunnally et al. using a GAD plasma for oxidative steam reforming of toluene and naphthalene [24]. Compared to the plasma tar reforming with no catalyst, the presence of the catalysts in the plasma reaction enhanced the conversion of tar model compounds and the energy efficiency simultaneously. The 7.5Ni7.5Co bimetallic catalyst exhibited the greatest activity of all three catalysts, showing the highest conversion of toluene (95.7%) and naphthalene (84.3%). The maximum energy efficiency for the conversion of toluene and naphthalene was 38.0 g/kWh and 2.3 g/kWh, respectively, achieved when coupling the 7.5Ni7.5Co catalyst with the GAD. In addition, the overall energy efficiency of the hybrid plasma tar reforming process was 40.3 g/kWh, 10.7 % higher than that using plasma-only.

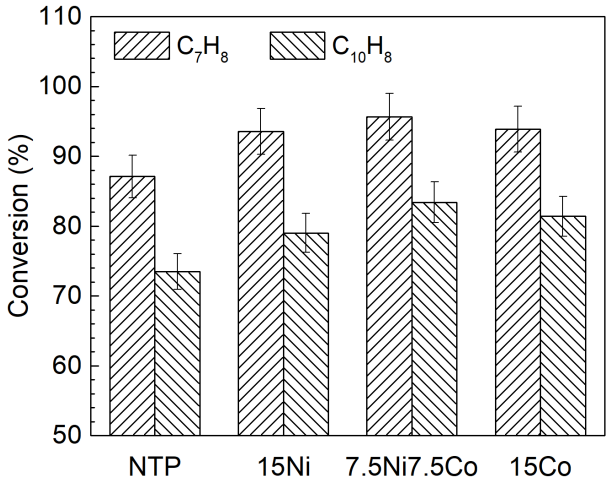

(a)

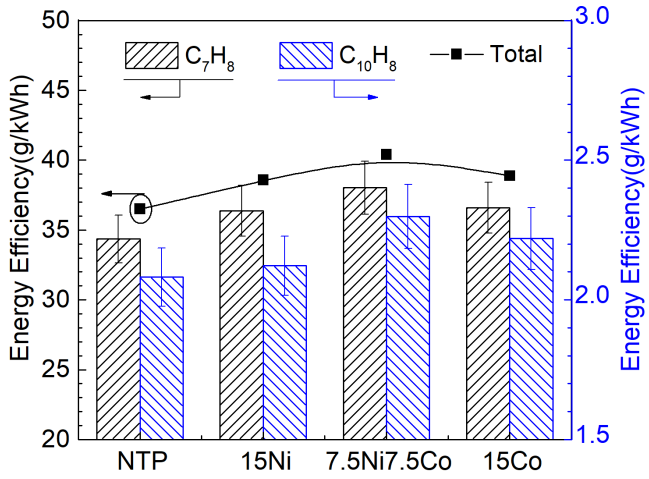

(b)

Fig.5. Effect of catalysts on (a) the conversion of toluene and naphthalene and (b) the energy efficiency for the conversion of toluene and naphthalene (C_7H_8 content: 15.0 g/Nm^3; $C_{10}H_8$ content: 1.0 g/Nm^3; Discharge power: 75 W; Q: 3.5 L/min; S/C molar ratio: 1.5).

In this study, the 7.5Ni7.5Co catalyst showed the best activity for the conversion of toluene and naphthalene in the plasma-catalytic tar reforming process, followed by the 15Co and the 15Ni catalysts. However, the specific surface area of these catalysts followed the order of 7.5Ni7.5Co > 15Ni > 15Co (Table 1), suggesting that the specific surface area of the catalysts might not be the determining factor in the plasma-catalytic conversion of toluene and naphthalene in this work. The effect of the catalysts on the conversion of tars agreed well with the reducibility of the catalysts followed the sequence of 7.5Ni7.5Co > 15Co > 15Ni, which indicates that the reducibility of the catalysts is closely associated to the conversion of tars.

In addition, the synergy between Ni and Co in the Ni-Co alloy would enhance the catalytic activity and reduce the coke deposition, and consequently improve the conversion of toluene and naphthalene [53, 54]. The enhanced reaction performance due to the Ni-Co bimetallic catalyst was also reported in thermal-catalytic reforming of hydrocarbons. Wang et al. performed thermal catalytic steam reforming of biomass tar (toluene) using Ni-Co catalysts in a continuous feeding dual-bed reactor [54]. They found that the steam reforming of toluene showed the highest conversion and the lowest coke formation using a 12Ni3Co/Al_2O_3 catalyst. Xiao et al. performed steam reforming of n-dodecane at 700 ^oC over Ce-promoted Ni-Co/Al_2O_3 catalysts in a fixed-bed tubular reactor [53]. The results indicated that the presence of the Ce-promoted Ni-Co/Al_2O_3 catalysts could enhance the catalytic activity and stability due to the formation of Ni-Co alloying. The highest conversion of n-dodecane (89%) was achieved using the 5 wt.% Ce-promoted 12Ni3Co/Al_2O_3 catalyst.

Fig. 6 shows the influence of the catalysts on the yield and selectivity of gaseous products. H_2, CO, C_2H_2, CO_2 and CH_4 were generated as the major gaseous products. Compared to the reforming reaction using plasma-only, the combination of GAD with the catalysts enhanced the yield of H_2 and CO in the following order: 7.5Ni7.5Co>15Co>15Ni, showing the same effect of the catalysts on the conversion of toluene and naphthalene (Fig. 4). The highest yield of H_2 (42.2%) and CO (37.3%) was achieved when using the 7.5Ni7.5Co catalyst, 49.5% and 33.3% higher than that using plasma-only, respectively. The coupling of GAD plasma with the 7.5Ni7.5Co catalyst also given the highest CO selectivity of 40.1%. In addition, the use of the catalysts had a limited effect on the selectivity (~1.7%) and yield (~1.5%) of CH_4, while both the yield and selectivity of C_2H_2 were reduced when using the catalysts. However, compared to the plasma tar reforming reaction without a catalyst, the coupling of GAD with these catalysts produced more CO_2, as shown by the enhanced selectivity and yield of CO_2. Note that the bimetallic catalyst (7.5Ni7.5Co) had the lowest selectivity and yield of CO_2 of all three catalysts. The formation of CO_2 could be ascribed to the occurrence of water gas shift reaction (R1) in the plasma reforming of toluene and naphthalene. Moreover, oxidative species (e.g., OH and O radicals) generated in the dissociation of water by electrons (R2 and R3) and excited

nitrogen species N_2^* (R4 and R5) might be able to further oxidize CO (R6 and R7) and the fragments of toluene and naphthalene into CO_2.

$$H_2O + CO \rightarrow CO_2 + H_2 \quad \text{(R1)}$$

$$H_2O + e \rightarrow H^- + OH \quad \text{(R2)}$$

$$H_2O + e \rightarrow 2H + O^- \quad \text{(R3)}$$

$$N_2 + e \rightarrow N_2^* + e \quad \text{(R4)}$$

$$H_2O + N_2^* \rightarrow N_2 + H + OH \quad \text{(R5)}$$

$$OH + CO \rightarrow CO_2 + H \quad \text{(R6)}$$

$$O + CO \rightarrow CO_2 \quad \text{(R7)}$$

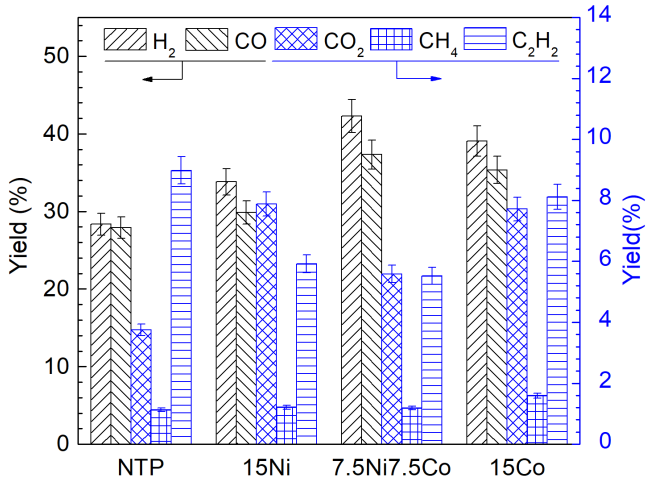

(a)

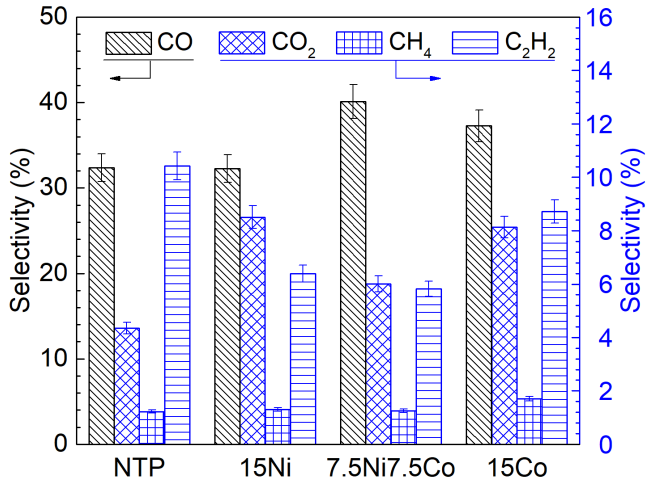

(b)

Fig. 6. Influence of catalysts on (a) the yield and (b) the selectivity of gas products (C_7H_8 content: 15.0 g/Nm^3; $C_{10}H_8$ content: 1.0 g/Nm^3; Discharge power: 75 W; Q: 3.5 L/min; S/C molar ratio: 1.5).

Thermal catalytic reforming of naphthalene and toluene was also carried out with all the conditions kept the same for the plasma reaction. However, there was almost no conversion of toluene and naphthalene at such a low reaction temperature (360 ^{o}C). These results indicate that a synergistic effect resulted from the coupling of GAD with catalysts was achieved as the reaction performance of the plasma-catalytic process was better than the sum of the plasma-only and catalyst-only.

Fig. 7 shows the influence of the catalysts on the synergistic capacity of the plasma-catalytic reforming of naphthalene and toluene. The 7.5Ni7.5Co catalyst showed the highest synergistic capacity for the conversion of tars, the energy efficiency, the selectivity of CO and the yield of H_2 and CO. The use of these catalysts reduced the formation of C_2H_2, giving a negative synergistic capacity of plasma-catalysis for C_2H_2 production.

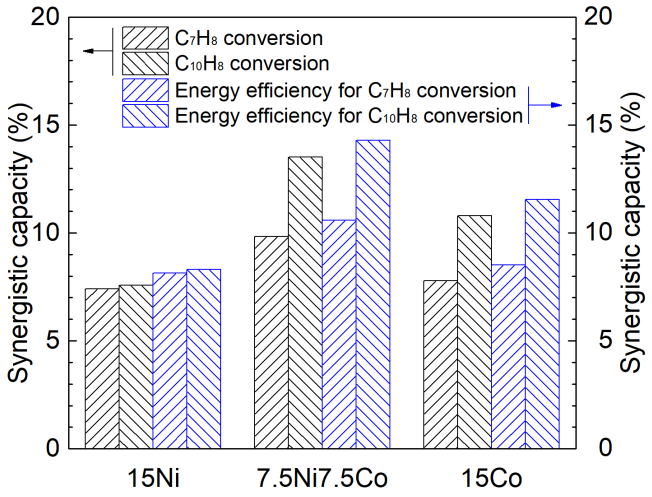

(a)

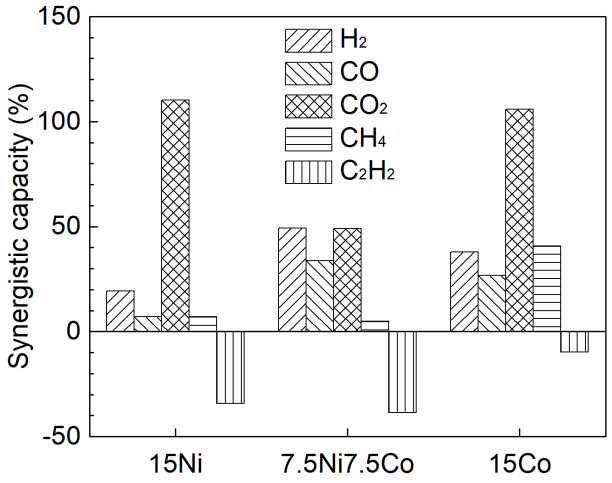

(b)

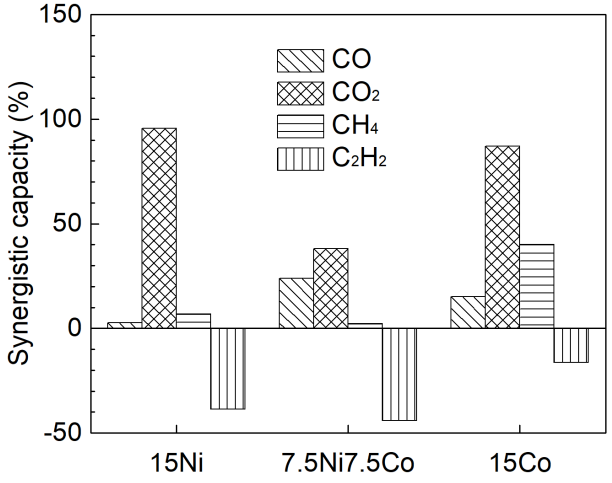

(c)

Fig. 7. Influence of catalysts on the synergistic capacity of plasma-catalytic reforming of mixed toluene and naphthalene: (a) tar conversion and energy efficiency; (b) yield of gas products; (c) selectivity of gas products (C_7H_8 content: 15.0 g/Nm^3; $C_{10}H_8$ content: 1.0 g/Nm^3; Discharge power: 75 W; Q: 3.5 L/min; S/C molar ratio: 1.5).

3.3 Reaction mechanism

The condensed by-products in the plasma reforming of mixed toluene and naphthalene were qualitatively analyzed by GC-MS, as listed in Table 2. Ethylbenzene, phenylethyne, styrene and benzene, 1-isocyano-2methyl were identified as the major by-products in both plasma-only and plasma-catalysis. N-containing chemicals (e.g., benzene,1-isocyano-2methyl) were found

in the plasma tar reforming without a catalyst, while the presence of the catalysts in the plasma reforming limited the formation of N-containing chemicals.

The initial destruction of toluene and naphthalene in the N_2 GAD can be induced via dissociation by energetic electrons and excited nitrogen species such as $N_2(A^3)$ and $N_2(a')$. Previous works showed that nitrogen metastable species make a significant contribution to the decomposition of low concentration pollutants (e.g., toluene and naphthalene) in N_2 plasmas [17][55]. The formation of aliphatic compounds (e.g.,1-butene, 3-methyl and oxalic acid) resulted from the breakage of C-C and C=C bonds in toluene and naphthalene molecules, and the subsequent recombination of their fragments. In the plasma reforming of mixed toluene and naphthalene, by-products (e.g., biphenyl and diphenyl ether) with a molecular weight larger than that of naphthalene were detected, suggesting the polymerization reaction occurred in the plasma reforming. However, the peak intensity of these by-products was several orders of magnitude lower than that of naphthalene, suggesting that the polymerization reaction can be neglected in the plasma tar reforming. Note that the combination of GAD and the catalysts significantly reduced the formation of by-products, as shown in Table 2. This phenomenon has also been observed in our previous work [16].

Table 2 By-products collected in the plasma steam reforming of toluene and naphthalene in plasma only and plasma catalysis processes.

No	Compound	Plasma-only	Plasma catalysis	No	Compound	Plasma-only	Plasma catalysis
1	1-Butene,3-methyl	√		10	Indene	√	
2	Oxalic acid	√	√	11	1,4-Dihydronaphthalene	√	√
3	Benzene	√		12	1-Methylnaphthalene	√	√
4	Ethylbenzene	√	√	13	Biphenyl	√	
5	O-xylene	√	√	14	1,4-Naphthoquinone	√	
6	Phenylethyne	√	√	15	Phthalic acid	√	√
7	Styrene	√	√	16	Acenaphthalene	√	

8	Benzene,1-isocyano-2methyl	√		17	Dibutyl phthalate	√	
9	Benzaldehydes	√		18	Diphenyl ether	√	

Plasma-catalytic reforming of mixed toluene and naphthalene is a complex process involving both gas phase reactions and surface reactions. The initial destruction of toluene and naphthalene in the gas phase can be induced via dissociation (R8-R11) by energetic electrons and excited nitrogen species such as $N_2(A^3)$ and $N_2(a')$, generating a range of free radicals (e.g., benzyl, phenyl, $CH_3^{\cdot}$, $C_6H_4CH_3^{\cdot}$, $C_{10}H_7^{\cdot}$ and $H^{\cdot}$) for the subsequent reactions. Previous works showed that nitrogen metastable species make a significant contribution to the decomposition of low concentration pollutants (e.g., toluene and naphthalene) in N_2 plasmas [17][55]. The formed OH radicals via water dissociation also contributed to the oxidation of toluene, naphthalene and their fragments (R12 and R13). In addition to H-addition reactions (R14-R16), the recombination of methyl with benzyl, phenyl and naphthyl formed ethylbenzene, o-xylene and 1-methylnaphthalene, respectively. In addition, styrene and phenylethyne could be generated via the stepwise dehydrogenation of ethylbenzene, while indene can be formed through the recombination of acetylene with benzyl followed by subsequent hydrogenation.

$$C_{10}H_8 + e \rightarrow C_8H_6 + C_2H_2 + e \quad \text{(R8)}$$

$$C_7H_8 + e \rightarrow C_5H_6 + C_2H_2 + e \quad \text{(R9)}$$

$$C_{10}H_8 + N_2^* \rightarrow C_8H_6 + C_2H_2 + N_2 \quad \text{(R10)}$$

$$C_7H_8 + N_2^* \rightarrow C_5H_6 + C_2H_2 + N_2 \quad \text{(R11)}$$

$$C_{10}H_8 + OH \rightarrow \text{Intermediates} + H_2O \quad \text{(R12)}$$

$$C_7H_8 + OH \rightarrow \text{Intermediates} + H_2O \quad \text{(R13)}$$

$$H + H \rightarrow H_2 \quad \text{(R14)}$$

$$CH_3 + H \rightarrow CH_4 \quad \text{(R15)}$$

$$H + C_6H_5 \rightarrow C_6H_6 \quad \text{(R16)}$$

In the plasma-catalytic tar reforming, toluene, naphthalene and other intermediates can be adsorbed onto the surfaces of the catalysts and reacted with active species (e.g., CH_x, OH and H radicals) formed in both the gas phase and on the catalyst surface. The combination of GAD with the catalysts thus provides additional reaction routes for the conversion of toluene and naphthalene, resulted in the enhanced conversion and hydrogen production.

3.4 Characterization of spent catalysts

Fig. 8 presents the TG results of the spent catalysts. The initial weight loss occurred at about 100 ^{o}C was due to thermal desorption of H_2O and adsorbed CO_2 [47]. The weight loss at around 240 ^{o}C and 440 ^{o}C was associated with the removal of carbonaceous species mainly consisting of oxidisable amorphous carbon [57], while the weight loss at a temperature >500 ^{o}C was related to the removal of whisker and graphitic carbon [58]. In this work, the temperature of the catalyst bed was around 360 ^{o}C, suggesting that most amorphous carbon could be re-oxidized in the plasma reaction, while the whisker and graphitic carbon was hard to be removed due to the relatively low reaction temperature in the reforming process and contributed to catalyst deactivation. Among the three catalysts, 7.5Ni7.5Co had the lowest carbon deposition (<4.5%) and was stable when running the plasma-catalytic reaction for 150 mins. The high carbon resistance of the 7.5Ni7.5Co catalyst can be mainly attributed to the formation of Ni-Co alloying on the catalyst surface due to the synergistic interaction between Ni and Co species.

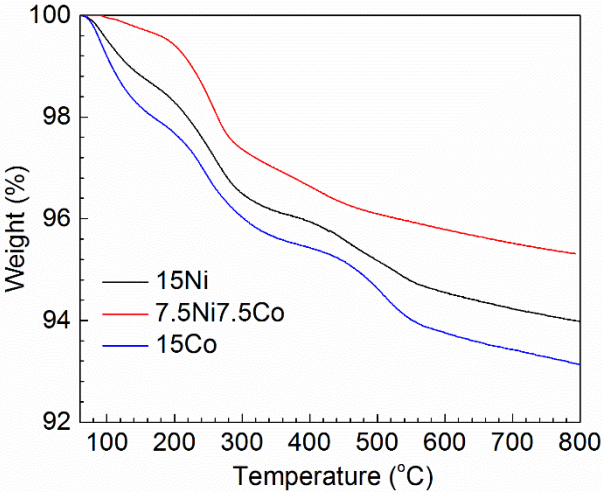

Fig. 8. TG results of the spent catalysts

3.5 Performance comparison for plasma-catalytic of tar conversion

Table 3 shows the conversion of typical tar model compounds (toluene and naphthalene) and corresponding energy efficiency using different plasma-catalytic reforming processes. Tao et al. reported that the combination of plasma with 0.5 g of Ni/SiO_2 catalyst greatly enhanced the conversion of toluene and energy efficiency of the process compared to the plasma reforming of toluene without a catalyst. However, the plasma reforming of toluene was carried out using He at a temperature of 773 K with extra heating [59]. Xu et al. investigated the reforming of toluene as a biomass tar surrogate over $Ni/\gamma\text{-}Al_2O_3$ in a temperature-controlled DBD plasma-catalytic reactor [23]. The effect of packing materials such as glass pellets and $\gamma\text{-}Al_2O_3$ pellets on the plasma reforming of toluene was evaluated. The highest energy efficiency of 38.8 g/kWh can be achieved for the conversion of toluene in fuel gas at a temperature of 673 K [23]. The proposed gliding arc PPC process showed promising performance with higher conversion and energy efficiency at a larger gas flow compared to other plasma systems, which can be partly attributed to higher electron density (~ 10^{23} m^{-3}) in gliding arc plasmas [38]. This value was comparable to the electron density of high-temperature thermal plasmas and was several orders of magnitude higher than that of corona discharges (10^{15} - 10^{19} m^{-3}) and DBD plasmas (10^{16} - 10^{19} m^{-3}) [38]. Developing novel coke-resistant catalytic materials with high activity and low

cost, and the optimization of GAD catalysis configuration has great potential to further enhance the energy efficiency of the plasma-catalytic tar reforming process.

Table 3 Performance comparison of reforming biomass tar by different technologies.

Processes	Tar	Working Gas	Tar Content (g/Nm^3)	Flow rate (m^3/h)	Specific energy input (kWh/m^3)	Conversion (%)	Energy efficiency (g/kWh)	References
Spark plasma reforming	C_7H_8	Humid He extra heating at 773 K S/C =1.0	258.6	0.0024	~7.2	34.0	12.2	[59]
Spark plasma + Ni/SiO_2 (IPC)						57.0	20.5	
DBD + γ-Al_2O_3 (IPC)	C_7H_8	Dry N_2 gas extra heating at 473 K	2.2	0.06	0.22	74.0	7.4	[23]
DBD + glass pellets (IPC)						55.0	5.5	
DBD + Ni/γ-Al_2O_3 (IPC)		Fuel gas extra heating at 673 K	4.4		0.10	88.2	38.8	
DBD + Ni/γ-Al_2O_3 (IPC)	C_7H_8	Humid Ar without extra heating S/C =2.5	17.7	0.015	2.33	47.1	2.6	[16]
AC GAD + Ni-Co/γ-Al_2O_3 (PPC)	C_7H_8/$C_{10}H_8$	Humid N_2 without extra heating S/C =1.5	16.0	0.21	0.38	95.1	40.3	This work

4. Conclusion

Steam reforming of mixed toluene and naphthalene over 15Ni, 7.5Ni7.5Co and 15Co was investigated in an AC gliding arc discharge plasma-catalysis reactor. Compared to the plasma reforming without a catalyst, the coupling of GAD with these catalysts enhanced the conversion and the energy efficiency of the hybrid process, while reduced the formation of by-products. The highest total tar conversion of 95.1% and energy efficiency of 40.3 g/kWh were achieved when using the 7.5Ni7.5Co catalyst, followed by the 15Ni and 15Co catalysts.

Compared to the plasma-only process, the yield of H_2 and CO in the plasma tar reforming combined with 7.5Ni7.5Co was greatly increased by 49.4% and 33.7%, respectively. In addition, the 7.5Ni7.5Co bimetallic catalyst also had the lowest carbon deposition on the catalyst surface. The superior performance of the 7.5Ni7.5Co bimetallic catalyst can be attributed to the formation of NiCo alloying on the catalyst surface due to the synergistic interaction between Ni and Co species.

Acknowledgement

The authors would like to acknowledge the financial support from the Royal Society Newton Advanced Fellowship (Ref. NAF/R1/180230), EPSRC Impact Acceleration Account (IAA), EPSRC SUPERGEN Bioenergy Challenge Programme (Ref. EP/M013162/1) and the Foundation of State Key Laboratory of Coal Combustion at Huazhong University of Science and Technology (No. FSKLCCB1805). We also acknowledge the European Union (EU) and Horizon 2020 funding awarded under the Marie Sklodowska-Curie action to the EUROPAH consortium (Grant number 722346).

Reference

[1] Z. Zhang, L. Liu, B. Shen, C. Wu, Preparation, modification and development of Ni-based catalysts for catalytic reforming of tar produced from biomass gasification, Renewable and Sustainable Energy Reviews, 94 (2018) 1086-1109.

[2] K. Qian, A. Kumar, Catalytic reforming of toluene and naphthalene (model tar) by char supported nickel catalyst, Fuel, 187 (2017) 128-136.

[3] M.A. Adnan, H. Susanto, H. Binous, O. Muraza, M.M. Hossain, Feed compositions and gasification potential of several biomasses including a microalgae: A thermodynamic modeling approach, International Journal of Hydrogen Energy, 42 (2017) 17009-17019.

[4] Y. Shen, J. Wang, X. Ge, M. Chen, By-products recycling for syngas cleanup in biomass pyrolysis – An overview, Renewable and Sustainable Energy Reviews, 59 (2016) 1246-1268.

[5] M.L. Valderrama Rios, A.M. González, E.E.S. Lora, O.A. Almazán del Olmo, Reduction of tar generated during biomass gasification: A review, Biomass and Bioenergy, 108 (2018) 345-370.

[6] S. Anis, Z.A. Zainal, Tar reduction in biomass producer gas via mechanical, catalytic and thermal methods: A review, Renewable and Sustainable Energy Reviews, 15 (2011) 2355-2377.

[7] B.S. Pathak, D.V. Kapatel, P.R. Bhoi, A.M. Sharma, D.K. Vyas, Design and development of sand bed filter for upgrading producer gas to IC engine quality fuel, Internaltional Energy Journal 8(2007) 15-20.

[8] L. Fagbemi, L. Khezami, R. Capart, Pyrolysis products from different biomasses: application to the thermal cracking of tar, Applied Energy, 69 (2001) 293-306.

[9] G. Guan, M. Kaewpanha, X. Hao, A. Abudula, Catalytic steam reforming of biomass tar: Prospects and challenges, Renewable and Sustainable Energy Reviews, 58 (2016) 450-461.

[10] D. Feng, Y. Zhao, Y. Zhang, S. Sun, S. Meng, Y. Guo, Y. Huang, Effects of K and Ca on reforming of model tar compounds with pyrolysis biochars under H_2O or CO_2, Chemical Engineering Journal, 306 (2016) 422-432.

[11] X.J. Liu, X.Q. Yang, C. Liu, P. Chen, X.M. Yue, S.Q. Zhang, Low-temperature catalytic steam reforming of toluene over activated carbon supported nickel catalysts, Journal of the Taiwan Institute of Chemical Engineers, 65 (2016) 233-241.

[12] M. Artetxe, M.A. Nahil, M. Olazar, P.T. Williams, Steam reforming of phenol as biomass tar model compound over Ni/Al_2O_3 catalyst, Fuel, 184 (2016) 629-636.

[13] D. Li, M. Tamura, Y. Nakagawa, K. Tomishige, Metal catalysts for steam reforming of tar derived from the gasification of lignocellulosic biomass, Bioresource Technology, 178 (2015) 53-64.

[14] T. Furusawa, K. Saito, Y. Kori, Y. Miura, M. Sato, N. Suzuki, Steam reforming of naphthalene/benzene with various types of Pt- and Ni-based catalysts for hydrogen production, Fuel, 103 (2013) 111-121.

[15] D. San-Jose-Alonso, J. Juan-Juan, M.J. Illan-Gomez, M.C. Roman-Martinez, Ni, Co and bimetallic Ni-Co catalysts for the dry reforming of methane, Applied Catalysis A-General, 371 (2009) 54-59.

[16] S.Y. Liu, D.H. Mei, M.A. Nahil, S. Gadkari, S. Gu, P.T. Williams, X. Tu, Hybrid plasma-catalytic steam reforming of toluene as a biomass tar model compound over Ni/Al_2O_3 catalysts, Fuel Processing Technology, 166 (2017) 269-275.

[17] S.Y. Liu, D.H. Mei, L. Wang, X. Tu, Steam reforming of toluene as biomass tar model compound in a gliding arc discharge reactor, Chemical Engineering Journal, 307 (2017) 793-802.

[18] D.H. Mei, B. Ashford, Y.-L. He, X. Tu, Plasma-catalytic reforming of biogas over supported Ni catalysts in a dielectric barrier discharge reactor: Effect of catalyst supports, Plasma Processes and Polymers, 14 (2017) 1600076.

[19] D.H. Mei, X.B. Zhu, Y.L. He, J.D. Yan, X. Tu, Plasma-assisted conversion of CO_2 in a dielectric barrier discharge reactor: understanding the effect of packing materials, Plasma Sources Science and Technology, 24 (2015) 015011.

[20] S.A. Nair, K. Yan, A.J.M. Pemen, E.J.M. van Heesch, K.J. Ptasinski, A.A.H. Drinkenburg, Tar removal from biomass derived fuel gas by pulsed corona discharges: Chemical kinetic study II, Industrial & Engineering Chemistry Research, 44 (2005) 1734-1741.

[21] W.F.L.M. Hoeben, F.J.C.M. Beckers, A.J.M. Pemen, E.J.M. van Heesch, W.L. Kling, Oxidative degradation of toluene and limonene in air by pulsed corona technology, Journal of Physics D-Applied Physics, 45 (2012).

[22] L.N. Liu, Q. Wang, S. Ahmad, X.Y. Yang, M.R. Ji, Y.F. Sun, Steam reforming of toluene as model biomass tar to H_2-rich syngas in a DBD plasma-catalytic system, Journal of the Energy Institute, 91 (2018) 927-939.

[23] B. Xu, J. Xie, H. Zhao, X. Yin, C. Wu, H. Liu, Removal of toluene as a biomass tar surrogate in a catalytic nonthermal plasma process, Energy & Fuels, 32 (2018) 10709-10719.

[24] T. Nunnally, A. Tsangaris, A. Rabinovich, G. Nirenberg, I. Chernets, A. Fridman, Gliding arc plasma oxidative steam reforming of a simulated syngas containing naphthalene and toluene, International Journal of Hydrogen Energy, 39 (2014) 11976-11989.

[25] H. Zhang, F. Zhu, X. Li, R. Xu, L. Li, J. Yan, X. Tu, Steam reforming of toluene and naphthalene as tar surrogate in a gliding arc discharge reactor, Journal of Hazardous Materials, 369 (2019) 244-253.

[26] Y. Wang, H. Yang, X. Tu, Plasma reforming of naphthalene as a tar model compound of biomass gasification, Energy Conversion and Management, 187 (2019) 593-604.

[27] J. Sun, Q. Wang, W. Wang, K. Wang, Plasma catalytic steam reforming of a model tar compound by microwave-metal discharges, Fuel, 234 (2018) 1278-1284.

[28] M. Wnukowski, P. Jamróz, Microwave plasma treatment of simulated biomass syngas: Interactions between the permanent syngas compounds and their influence on the model tar compound conversion, Fuel Processing Technology, 173 (2018) 229-242.

[29] J. Van Durme, J. Dewulf, C. Leys, H. Van Langenhove, Combining non-thermal plasma with heterogeneous catalysis in waste gas treatment: A review, Applied Catalysis B-Environmental, 78 (2008) 324-333.

[30] J.C. Whitehead, Plasma catalysis: A solution for environmental problems, Pure and Applied Chemistry, 82 (2010) 1329-1336.

[31] L. Wang, Y. Yi, H. Guo, X. Tu, Atmospheric pressure and room temperature synthesis of methanol through plasma-catalytic hydrogenation of CO_2, ACS Catalysis, 8 (2017) 90-100.

[32] L. Wang, Y. Yi, C. Wu, H. Guo, X. Tu, One-step reforming of CO_2 and CH_4 into high-value liquid chemicals and fuels at room temperature by plasma-driven catalysis, Angewandte Chemie International Edition, 56 (2017) 13679-13683.

[33] F.S. Zhu, H. Zhang, X. Yan, J. Yan, M. Ni, X. Li, X. Tu, Plasma-catalytic reforming of CO_2 -rich biogas over Ni/γAl_2O_3 catalysts in a rotating gliding arc reactor, Fuel, 199 (2017) 430-437.

[34] A.A. Assadi, S. Loganathan, P.N. Tri, S. Gharib-Abou Ghaida, A. Bouzaza, A.N. Tuan, D. Wolbert, Pilot scale degradation of mono and multi volatile organic compounds by

surface discharge plasma/TiO_2 reactor: Investigation of competition and synergism, Journal of Hazardous Materials, 357 (2018) 305-313.

[35] H. Zhang, F. Zhu, X. Li, K. Cen, C. Du, X. Tu, Enhanced hydrogen production by methanol decomposition using a novel rotating gliding arc discharge plasma, RSC Advances, 6 (2016) 12770-12781.

[36] D.H. Mei, X.B. Zhu, C.F. Wu, B. Ashford, P.T. Williams, X. Tu, Plasma-photocatalytic conversion of CO_2 at low temperatures: Understanding the synergistic effect of plasma-catalysis, Applied Catalysis B: Environmental, 182 (2016) 525-532.

[37] X. Tu, H.J. Gallon, J.C. Whitehead, Plasma-assisted reduction of a NiO/Al_2O_3 catalyst in atmospheric pressure H_2/Ar dielectric barrier discharge, Catalysis Today, 211 (2013) 120-125.

[38] X. Tu, J.C. Whitehead, Plasma dry reforming of methane in an atmospheric pressure AC gliding arc discharge: Co-generation of syngas and carbon nanomaterials, International Journal of Hydrogen Energy, 39 (2014) 9658-9669.

[39] F. Saleem, K. Zhang, A. Harvey, Plasma-assisted decomposition of a biomass gasification tar analogue into lower hydrocarbons in a synthetic product gas using a dielectric barrier discharge reactor, Fuel, 235 (2019) 1412-1419.

[40] K. Li, J.-L. Liu, X.-S. Li, X. Zhu, A.-M. Zhu, Warm plasma catalytic reforming of biogas in a heat-insulated reactor: Dramatic energy efficiency and catalyst auto-reduction, Chemical Engineering Journal, 288 (2016) 671-679.

[41] T. Hammer, T. Kappes, M. Baldauf, Plasma catalytic hybrid processes: gas discharge initiation and plasma activation of catalytic processes, Catalysis Today, 89 (2004) 5-14.

[42] Y. Zeng, X. Tu, Plasma-catalytic hydrogenation of CO_2 for the cogeneration of CO and CH_4 in a dielectric barrier discharge reactor: effect of argon addition, Journal of Physics D: Applied Physics, 50 (2017) 184004.

[43] K. Ray, S. Sengupta, G. Deo, Reforming and cracking of CH_4 over Al_2O_3 supported Ni, Ni-Fe and Ni-Co catalysts, Fuel Processing Technology, 156 (2017) 195-203.

[44] H. Zhang, F. Zhu, Z. Bo, K. Cen, X. Li, Hydrogen production from methanol decomposition in a gliding arc discharge plasma with high processing capacity, Chemistry Letters, 44 (2015) 1315-1317.

[45] L. Zhou, L. Li, N. Wei, J. Li, J.-M. Basset, Effect of $NiAl_2O_4$ Formation on Ni/Al_2O_3 stability during dry reforming of methane, ChemCatChem, 7 (2015) 2508-2516.

[46] C.-B. Wang, C.-W. Tang, H.-C. Tsai, S.-H. Chien, Characterization and catalytic oxidation of carbon monoxide over supported cobalt catalysts, Catalysis Letters, 107 (2006) 223-230.

[47] X.X. Zhao, G.X. Lu, Modulating and controlling active species dispersion over Ni-Co bimetallic catalysts for enhancement of hydrogen production of ethanol steam reforming, International Journal of Hydrogen Energy, 41 (2016) 3349-3362.

[48] X.J. You, X. Wang, Y.H. Ma, J.J. Liu, W.M. Liu, X.L. Xu, H.G. Peng, C.Q. Li, W.F. Zhou, P. Yuan, X.H. Chen, Ni-Co/Al_2O_3 bimetallic catalysts for CH_4 steam reforming: Elucidating the role of Co for improving coke resistance, Chemcatchem, 6 (2014) 3377-3386.

[49] S. Sengupta, K. Ray, G. Deo, Effects of modifying Ni/Al_2O_3 catalyst with cobalt on the reforming of CH_4 with CO_2 and cracking of CH_4 reactions, International Journal of Hydrogen Energy, 39 (2014) 11462-11472.

[50] V.M. Gonzalez-delaCruz, R. Pereniguez, F. Ternero, J.P. Holgado, A. Caballero, In Situ XAS Study of Synergic Effects on Ni-Co/ZrO_2 Methane Reforming Catalysts, Journal of Physical Chemistry C, 116 (2012) 2919-2926.

[51] J.K. Xu, W. Zhou, Z.J. Li, J.H. Wang, J.X. Ma, Biogas reforming for hydrogen production over nickel and cobalt bimetallic catalysts, International Journal of Hydrogen Energy, 34 (2009) 6646-6654.

[52] S. Andonova, C.N. de Ávila, K. Arishtirova, J.M.C. Bueno, S. Damyanova, Structure and redox properties of Co promoted Ni/Al_2O_3 catalysts for oxidative steam reforming of ethanol, Applied Catalysis B: Environmental, 105 (2011) 346-360.

[53] Z.R. Xiao, L. Li, C. Wu, G.Z. Li, G.Z. Liu, L. Wang, Ceria-promoted Ni-Co/Al_2O_3 catalysts for n-dodecane steam reforming, Catalysis Letters, 146 (2016) 1780-1791.

[54] L. Wang, D. Li, M. Koike, H. Watanabe, Y. Xu, Y. Nakagawa, K. Tomishige, Catalytic performance and characterization of Ni–Co catalysts for the steam reforming of biomass tar to synthesis gas, Fuel, 112 (2013) 654-661.

[55] A.N. Trushkin, I.V. Kochetov, Simulation of toluene decomposition in a pulse-periodic discharge operating in a mixture of molecular nitrogen and oxygen, Plasma Physics Report+, 38 (2012) 407-431.

[56] U. Oemar, A. Ming Li, K. Hidajat, S. Kawi, Mechanism and kinetic modeling for steam reforming of toluene on $La_{0.8}Sr_{0.2}Ni_{0.8}Fe_{0.2}O_3$catalyst, AIChE Journal, 60 (2014) 4190-4198.

[57] W. Nabgan, T.A.T. Abdullah, R. Mat, B. Nabgan, A.A. Jalil, L. Firmansyah, S. Triwahyono, Production of hydrogen via steam reforming of acetic acid over Ni and Co supported on La_2O_3 catalyst, International Journal of Hydrogen Energy, 42 (2017) 8975-8985.

[58] X. Huang, C.C. Jia, C.Z. Wang, F.K. Xiao, N. Zhao, N.N. Sun, W. Wei, Y.H. Sun, Ordered mesoporous CoO-NiO-Al_2O_3 bimetallic catalysts with dual confinement effects for CO_2 reforming of CH_4, Catalysis Today, 281 (2017) 241-249.

[59] K. Tao, N. Ohta, G.Q. Liu, Y. Yoneyama, T. Wang, N. Tsubaki, Plasma enhanced catalytic reforming of biomass tar model compound to syngas, Fuel, 104 (2013) 53-57.